

THERMO-MECHANICAL AND STRUCTURAL PROPERTIES OF A LOW DEGREE POLYNOMIAL EMBEDDED ATOMS MODEL METAL

I. STANKOVIĆ*, M. KRÖGER** AND S. HESS*

* *Institute of Theoretical Physics, PN 7-1, TU Berlin, D-10623 Berlin, Germany*

** *Polymer Physics, Material Sciences, ETH Zurich, CH-8092 Zurich, Switzerland*

ABSTRACT

The low degree polynomial embedded atom model is adapted to study the thermo-mechanical behaviour and structure of model metals with non-equilibrium molecular dynamics simulations. The main constitutive properties, e.g. elastic coefficients, cohesive energy and lattice constant, of real metals can be reproduced by a set of basic model potentials as revealed by analytic considerations at zero temperature. The model is used to study systematically the behaviour of qualitatively similar, but quantitatively different systems under shear. The influence of elastic moduli and structure at finite temperature on shear stress is discussed. Further, in the case of mismatch between preferred local and the global embedding densities, formation of metallic sponges is observed. We analyze the time evolution of the sponges for different values of cohesive and surface energies.

Keywords: embedded particle, molecular dynamics, metal, friction, sponge, diffusion

1. Introduction

Metals have been subject of numerical simulations since the earliest availability of digital computers for scientific computing. The embedded atom method was originated by Daw and Baskes [1] and views each particle as "embedded" in host lattice of all other particles, complying with the fact that in real metals conducting electrons are not localized about nuclei and total energy depends upon local electron density. A particularly simple choice of model, the "generic embedded atom model" (GEAM), will be shown to reproduce the main zero-temperature constitutive properties of real metal by varying a set of basic model parameters: the strength of the embedding function, the position of the minimum and the cut-off radius. The model parameters independently adjust several constitutive properties (elastic coefficients, lattice constant and cohesive energy) allowing a systematic analysis of the influence of constitutive properties thermo-mechanical behaviour of metals. In particular, only the 'quadratic term' in the embedding functional contributes to the elastic coefficients that include response to volume changing deformation (bulk modulus B , C_{11} and C_{12}) since they depend on the second derivative of the cohesive energy. The nonequilibrium molecular dynamics (NEMD) simulations are used to study the influence of temperature and shear rate on stress tensor in viscoplastic (strong) flow regime.

Crystalline materials and metals undergo significant structural transformations on a range of length scales when subjected to steady shear flow [2,3]. Dry solid friction of two metal bodies involves the formation, growth, and disappearance of a number of small contact zones (asperities, area typically of the order of $10\mu\text{m}^2$ while occupying 0.1% of the visible area), in which friction forces are thought to build up [4]. Low energy electron diffraction (LEED) reveals structural changes, originated by large relative speeds in the surface layers -- at a moderate overall speed -- may propagate over several thousands crystal lattice constants [3]. Thus, the frictional force -- the shear stress integrated over the volume of the asperities -- must be considered as inhomogeneous with respect to density, velocity, and temperature fields.

Further, the proposed model for a bulk metal is used to obtain metallic sponges and porous metal structures with wide range of porosities. We demonstrate an application of the model metal sponge to study diffusion of a gas of short ranged attractive (SHRAT) particles in porous medium.

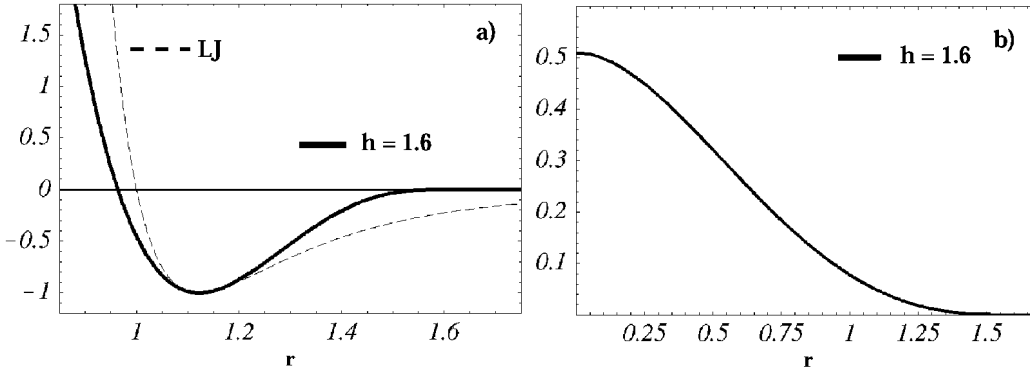


Fig. 1 The binary interaction potential (a) used in the NEMD simulations (bold) is plotted together with a Lennard-Jones (dashed, LJ) potential, both in dimensionless LJ units. The potential cut-off ($r_{cut}=h=1.6r_0$) and minima ($r_{min}=r_{min}^{LJ}=2^{1/6} r_0$) are model parameters. The Lucy weight function $w(r)$ used to calculate embedding density (b).

2. Embedded atom model

The embedded atom model potential is the sum of two contributions to the total potential energy E : a conventional binary interaction term through a two-body interaction potential U and a term stemming from an embedding functional F , which models the effect of the electronic 'glue' between atoms localized about the nuclei [1],

$$E = \sum_{i=1}^N (F(\rho_i) + \sum_{j>i}^N U(r^{ij})) \quad (1)$$

where N is number of atoms at positions $\mathbf{r}^i=1,2,\dots,N$ and r^{ij} is the norm of the relative vector $\mathbf{r}^{ij}=\mathbf{r}^i-\mathbf{r}^j$ between atoms i and j . The energy depends upon the local embedding density ρ_i , resulting in forces between ions that are many body in character, rather than simply pairwise additive. In our GEAM model for the binary potential function U we use a radially symmetric short ranged attractive potential (Fig. 1a) [5]:

$$U(r) = \phi_0 r_0^{-4} (3(r_{cut} - r)^4 - 4(r_{cut} - r_{min})(r_{cut} - r)^3), \quad r \leq r_{cut} \quad (2)$$

and $U(r)=0$ otherwise, with an energy scale ϕ_0 , a length scale r_0 , an interaction range r_{min} , and a smooth cut-off radius r_{cut} . The well depth of the two-particle (binary interaction) potential U is $U(r_{min}) = -\phi_0 r_0^{-4} (r_{cut} - r_{min})^4$. This format of the potential has been recently used as the effective two-particle interaction in the embedded atom model metal [5,6,7], and to model thermophysical properties of fluids and solids [8]. The embedding potential in polynomial form for GEAM is:

$$F(\rho) = \phi_0 \sum_{k=2,4,\dots} F_k ((\rho - \rho_{des})^k - (w_0 - \rho_{des})^k) r_0^{3k} \quad (3)$$

where ρ_{des} is the desired embedding number density and F_k are embedding strengths, being part of the model. The local embedding density ρ_i is constructed from the radial coordinates of surrounding atoms and requires the choice of a weighting function $w(r)$, $\rho_i = \sum_{j \neq i} w(r^{ij}) + w(0)$. For reasons discussed in [5,9] we use the normalized Lucy's weight function (see Fig. 1b):

$$w(r) = w_0 (1 + 3r/r_{cut})(1 - r/r_{cut}), \quad r \leq r_{cut} \quad (4)$$

with $w_0=w(0)=105/(16\pi r_{cut})$. Throughout this work, we investigate the 'basic' GEAM model metal for which the desired density $\rho_{des}=r_0^{-3}$ equals the particle number density $n=N/V=r_0^{-3}$; $F_0=1$, $r_{min}=2^{1/6} r_0$ and $r_{cut}=1.6r_0$ are fixed.

Like a Lennard-Jones potential, the GEAM will be used to study the behaviour of qualitatively similar, but quantitatively different systems. To do that, we will exploit the property of its polynomial format, to allow systematical varying of one constitutive property while other constitutive properties remain largely unchanged.

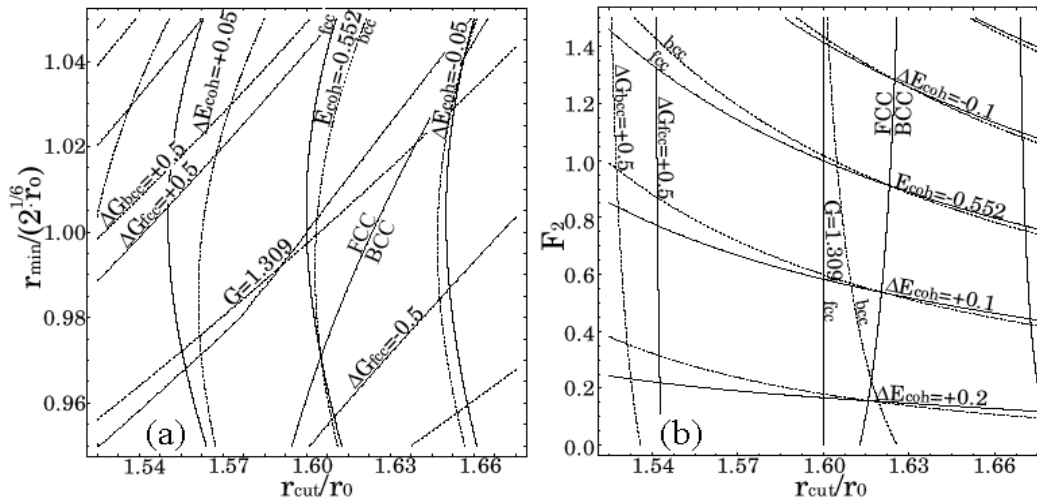


Fig. 2 Cohesive energy E_{coh} and shear modulus G for the case of vanishing pressure tensor. All quantities are in standard LJ units. Line, that separates areas where bcc/fcc structures are energetically preferred, is plotted. Values for fcc (solid curves) and bcc (dashed curves) structure are presented. (a) Effect of cut-off radius r_{cut} , position of the potential minimum r_{min} for $F_2=1$ (GEAM). (b) Effect of cut-off radius r_{cut} , and embedding strength F_2 for $r_{min}=2^{1/6}r_0$ (GEAM).

The energy per particle can be calculated from Eq. 1 for particles, which occupy ideal lattice sites. In present model, face centred cubic (fcc) and hexagonal close packed (hcp) structures are energetically equivalent for $n^{-1/3}r_{cut}r_0 < 1.83$. For densities close to $n^{-1/3}r_0=1$ the minimum energy is lower in fcc solids. In order to describe the influence of model parameters on some constitutive properties of ideal fcc and bcc structures we will consider a state point with vanishing (total) isotropic pressure and fix the binary potential well depth to the above GEAM value. Changing the values r_{min} and r_{cut} controls the shape of the binary potential. The size of r_{cut} changes the strength of contributions to the embedding density. The corresponding parameter in other embedded atom models, cf. Refs. [9], is the nearest neighbour equilibrium distance. In the following, elastic coefficients, pressure tensor and related quantities are evaluated from the expressions given in the previous section in the limit of low temperatures, where particles occupy ideal lattice sites.

The cohesive energy $E_{coh}=E/N$, or energy per particle, depends strongly on the embedding part of the model potential; see Fig.2a, b for a quantitative analysis. At larger values of r_{cut} body centred cubic structure (fcc) is energetically preferred (Fig.2a). The main contribution of the two-particle interaction to E_{coh} stems from the first neighbours. At zero pressure, the first neighbours are near the minimum of the binary potential; the resulting density depends only on the position of the minimum of the potential. Since the well depth of the two-particle potential is held constant, the cohesive energy does not depend on the position of the potential minimum, cf. Fig.2a. The cohesive energy depends stronger on embedding strength parameters ($F_k, k=2,4,\dots$) then on size of cut-off radius r_{cut} .

The elastic coefficients - bulk modulus B , (average) shear modulus G , C_{44} and the Cauchy pressure $(C_{11}-C_{12})/2$ depend on the second derivative of the free energy for a nearest neighbour model [10]. The second order term ($k=2$, Eq. 3) in the embedding functional is most important for the values of the elasticity coefficients which include response of material on volume changes (B, C_{11}, C_{12}) since the embedding density is very close to the desired embedding density. Shear, C_{44} and Cauchy pressure moduli in cubic crystals include only response to volume conserving shear deformation that do not change embedding density and consequently contribution of embedding functional to free energy. For this reason shear moduli depend only on two body interaction parameters (r_{min}, r_{cut}) see Fig. 2a,b. This enables us to fit experimental values for the shear moduli G and bulk moduli B independently by varying strength of F_2 term. Other order terms of embedding functional ($F_k, k \geq 4$) may be considered to obtain an improved quantitative agreement between model behaviours and experimentally observed behaviours, in particular with respect to the ratios between elastic coefficients and cohesive energy.

3. Nonequilibrium molecular dynamics simulation method and reference values

The equations of motion are integrated with a standard velocity-Verlet algorithm with a force acting on particle i : $F_i = -\sum_{j \neq i} (\partial\Phi/\partial\mathbf{r}_{ij} + (\partial F/\partial\rho_i + \partial F/\partial\rho_j)\partial w/\partial\mathbf{r}_{ij})$ obtained directly from eq. (1) by variation of energy. Suitable integration step is $\Delta t/t_{ref}=0.01$. A cubic simulation box with constant volume and Lees-Edwards periodic boundary conditions are used to simulate shear deformation. The profile unbiased thermostat with rescaling of velocities (which corresponds to Gaussian constraint) is used to control temperature. For more details on simulation method see Ref. [11].

To compare NEMD simulation results with experimental data, we relate constitutive properties of our model with experimental data. Any measurable quantity Q with a dimension $[Q]$ specified in SI units kg, m and s is made

dimensionless by a reference quantity $Q_{\text{ref}}=m^{\alpha+\gamma/2}r_0^{\beta+\gamma}\phi_0^{-\gamma/2}$ for $[Q]=\text{kg}^\alpha\text{m}^\beta\text{s}^\gamma$ such that $Q=Q_{\text{dimless}}Q_{\text{ref}}$ quantities m , r_0 and ϕ_0 provide the scales via the interaction potential Eq. 1-4 and the equations of motion. The reference values for length r , number density n , energy $k_B T$, temperature T , time t , shear rate $\dot{\gamma}$, pressure P and the elastic moduli in terms of the simulation parameters are therefore $r_{\text{ref}}=r_0$, $n_{\text{ref}}=r_0^{-3}$, $e_{\text{ref}}=\phi_0=k_B T_{\text{ref}}$, $t_{\text{ref}}=r_0(m/\phi_0)^{1/2}$ and $P_{\text{ref}}=\phi_0 r_0^{-3}=e_{\text{ref}} n_{\text{ref}}$. For Cu, e.g., one obtains reference values $\phi_0=3.61\text{eV}$ and $P_{\text{ref}}=38\text{GPa}$, $r_0=2.26\text{\AA}$, and $n_{\text{ref}}=86.2\text{nm}^{-3}$. Atomic mass of copper is $m_{\text{Cu}}=1.06\cdot 10^{-22}\text{kg}$ and the reference time is estimated as $t_{\text{ref}}=0.97\cdot 10^{-13}\text{s}$. By choosing $T_{\text{ref}}=40\text{kK}$, $P_{\text{ref}}=40\text{GPa}$ one obtains $\phi_0=3.45\text{eV}$, $n_{\text{ref}}=72.5\text{nm}^{-3}$ and $r_0=2.4\text{\AA}$ for GEAM.

4. Rheological properties of GEAM metal in stationary strong flow

For a planar Couette flow, which corresponds to stationary flow regime, the symmetric traceless pressure tensor has only three independent components $p_{+,-,0}$, a shear pressure $p_{+}=P_{xy}$ or shear stress $-P_{xy}$, and two normal pressure differences: $P_{-}=(P_{xx}-P_{yy})/2$, $p_0=2P_{zz}-(P_{xx}+P_{yy})/4$. We calculate via NEMD simulations with 43000 particles the pressure tensor over the range of temperatures $T=0.008, \dots, 0.06$, for densities $n=0.98, \dots, 1.08$, and for two shear rates $\dot{\gamma}=0.001, 0.01$.

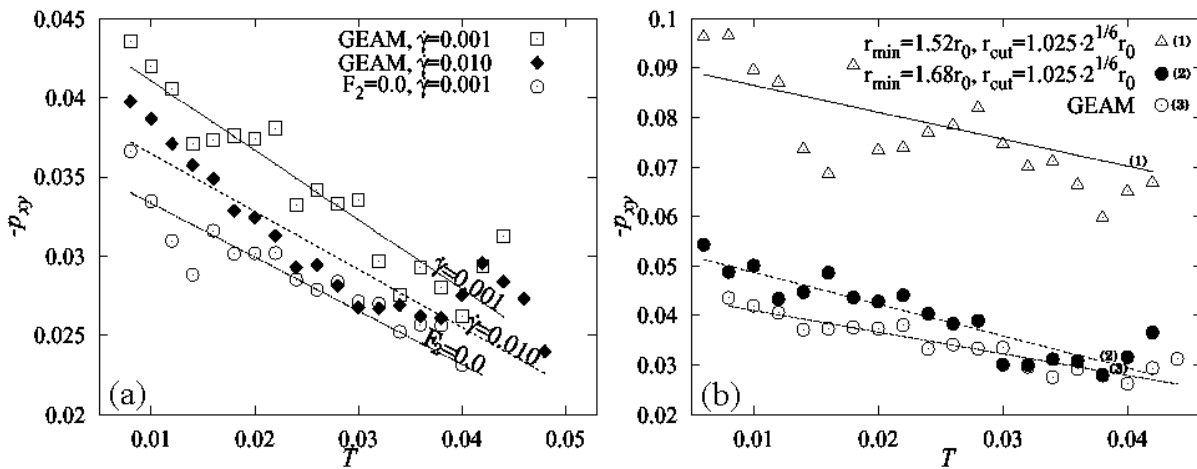


Fig. 3 Shear stress vs. temperature: a) Symbols denote averages from the NEMD simulation of GEAM with different densities for two shear rates $\dot{\gamma}=0.001, 0.01$ ($F_2=1$) and for $F_2=0$ ($\dot{\gamma}=0.001$). b) Results for different model parameters, cut-off r_{cut} and minimum of the potential r_{min} . All quantities are expressed in LJ units. Curves are obtained by linear regression analysis of the simulation results.

In order to discuss the relationship between shear stress and temperature for two shear rates we test a simple linear relationship between them, where the coefficients are obtained via regression. Within statistical errors and for the range of chosen densities, we did not detect an effect of density on the friction pressure. The regression curves of shear stress ($-P_{+}$ or $-P_{xy}$) together with the simulation data are presented in Fig. 3a. Data are plotted for two shear rates $\dot{\gamma}=0.001, 0.010$. The shear stress decreases with increasing temperature. This is so, because atoms have large kinetic energies and can move uncorrelated and far from their equilibrium positions as compared to atoms in a layer plane. For the same reason, the observed shear stress decreases with increasing shear rate (Fig.3. left). At a higher shear rate more defects are produced and the ordering of atoms into hexagonal layers is weakened [9]. The embedding contribution reduces density fluctuations, making atoms more bounded into layer structure, thus shear stress decreases with decreasing influence of embedding contribution. The simulated values of the two normal pressure differences $p_{-,0}$ are found to both vanish within the precision of our data.

In Fig. 3b, the data are presented for three systems: GEAM (with fcc ground state structure and shear moduli $G=1.31$), for model parameters: $r_{\text{min}}=1.025\cdot 2^{1/6}$, $r_{\text{cut}}=1.68$, $F_2=1$ (bcc, $G=1.33$) and $r_{\text{min}}=1.025\cdot 2^{1/6}$, $r_{\text{cut}}=1.52$, $F_2=1$ (fcc, $G=2.39$). Since the shear stress and moduli have the same origin in shape of two-body interaction potential, the observed shear stress increases linearly with increase of the shear moduli. The dependencies of shear stress on temperature and shear rate are particularly important when the metal is subject to severe stresses or non-uniform heating, e.g., as result of thread-breaking [3].

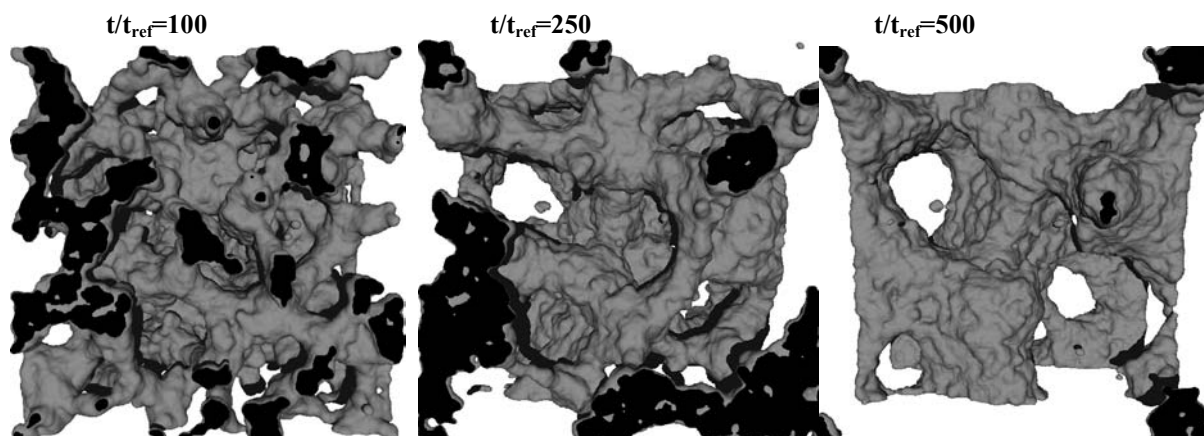


Fig. 4. Equilibration of a GEAM metal sponge at $T/T_{ref}=0.04$ ($N=50000$, $n=0.25$, $\rho_{des}=1$, all in reduced units) obtained via MD simulation. Initial configuration: fcc lattice (not shown). Snapshots taken at $t/t_{ref}=100$ (left), 250 (middle) and 500 (right).

5. Diffusion in porous structures (sponges)

To create metallic sponge we introduce controlled mismatch between overall number density $n=N/V=0.25$ in reduced units and desired (bulk, wall) embedding density $\rho_{des}=1.0$ of the GEAM metal. Evolution of a model metal sponge is shown in Fig. 4. The model metal tries to microphase-separate such that the local embedding density approaches the desired value (ρ_{des}). Surface tension in the GEAM metal tries to reduce surface of the sponge and keeps the sponge walls connected. This results in decreasing porosity of the structure. A comparison with systems, which are smaller/larger by factor 10-20, confirms that the sponge structure is qualitatively independent of system size above $N \approx 10000$ particles under the current conditions.

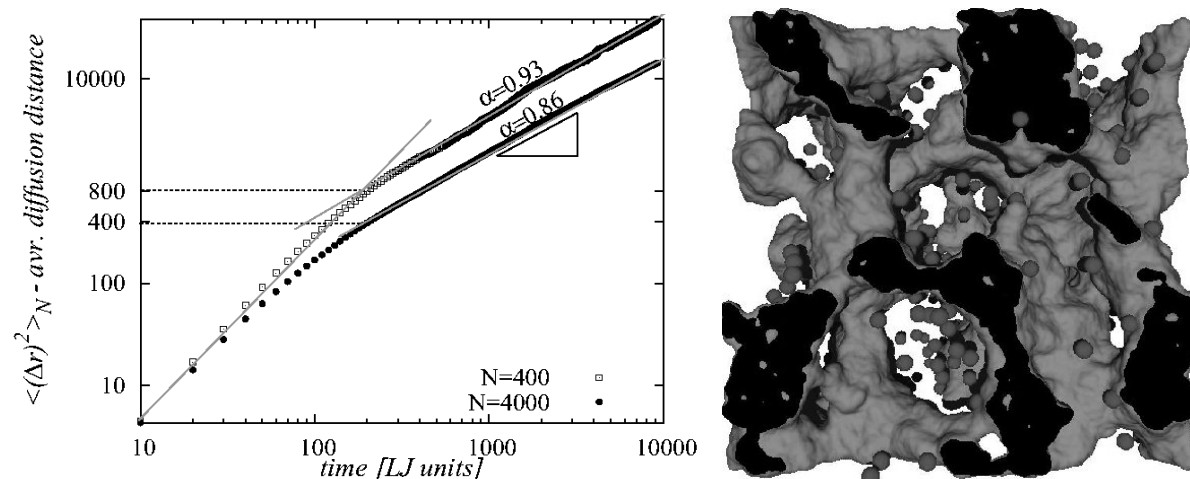


Fig. 5. Mean square displacement (average diffusion distance) of SHRAT particle gas inside of the GEAM matrix at temperature $T/T_{ref}=0.01$, for $N=400, 4000$ SHRAT particles (left). Snapshot of the system with $N=400$ SHRAT particles at $t/t_{ref}=900$ (right). The GEAM metal sponge is fixed at $t/t_{ref}=250$, $n/n_{ref}=0.25$ and $N_{GEAM}=50000$.

An example of GEAM metal sponge application is shown in Fig. 5. The sponge is filled with particles interacting with each other through SHRAT potential (Eq. 2), and interaction between wall and gas particles is repulsive with smooth cut-off at r_{min} : $\Phi(r)=\phi_0 r_0^{-4}(r_{min}-r)^4$, $r \leq r_{min}$ and $\Phi(r)=0$ otherwise. Gas is thermostated indirectly through the collisions with the sponge wall particles. Temperature of the particles at the sponge surface is controlled by rescaling of their velocities [11], while positions of particles inside of the sponge are fixed to stabilize the structure and prevent a change of its porosity during the simulation. In Fig. 5, molecular

dynamics results are given at temperature $T/T_{\text{ref}}=0.01$ for dilute SHRAT gas with $N=400, 4000$ particles. Collision (free flight) time, $t_{\text{coll}} \approx 110$, in smaller system ($N=400$) is determined by typical pore diameter $R_{\text{coll}} \approx 24$. For $N=4000$ collision time is shorter, $t_{\text{coll}} \approx 40$, due to the SHRAT-SHRAT particle interactions. We observe clusters of SHRAT particles formed during the simulation. For this reason at times larger than collision time, the mean square displacement increases with curvature $\alpha=0.86, 0.93$ for systems with $N=400, 4000$ particles respectively. In systems where particles move randomly, one would expect $\alpha=1$, according to Einstein relation, $\langle \Delta r^2 \rangle = 6Dt$.

6. Conclusion

The embedded atom method has been applied to study thermo-mechanical behaviour of the model GEAM metal. The constitutive properties (cohesive energy, lattice constant and elasticity coefficients) of real metals are reproduced by a set of basic model parameters: position of potential minima, cut-off radius and strength of embedding functional. Application of embedded atom method to simulations of shear flow of model metal and dry solid friction is presented. Under the appropriate choice of simulation parameters (controlled mismatch between desired embedding density and number density), the model turns out also to be applicable for studying multiscale structure of porous media. The metallic porous structures are an ideal matrix to be filled with fluid, and to study, e.g., transport and diffusion in porous materials.

Authors gratefully acknowledge financial support by Deutsche Forschungsgemeinschaft (DFG) through special research project (Sfb) 448 'Mesoskopisch strukturierte Verbundsysteme'.

7. References:

- [1] M. S. Daw and M. I. Baskes, Phys. Rev. Lett. **50**, 1983, p.1285; Phys. Rev. B **29**, 1984, p. 6443.
- [2] Friction and Rheology on the Nanometer Scale E. Meyer, T. Gyalog, R. M. Overney, and K. Fransfeld, Eds., (World Scientific, Singapore, 1998); M. Braun and M. Peyrard, Phys. Rev. E **63**, 2001, 046110; M. H. Müser and M. O. Robbins, Phys. Rev. B **61**, 2000, p. 2335.
- [3] F. P. Bowden and D. Tabor, The friction and lubrication of solids, 2nd Ed. (Clarendon Press, Oxford, 1954); V. D. Scott and T. Wilman, Proc. Roy. Soc. **247**, 1958, p. 353.
- [4] B. N. J. Persson, Sliding Friction, 2nd Ed. (Springer, Berlin, 2002); B.N.J. Persson, F. Bucher, and B. Chiaia, Phys. Rev. B **65**, 2002, 184106.
- [5] W. G. Hoover and S. Hess, Physica A **267**, 1999, p. 98.
- [6] M. Kröger and S. Hess, Z. Angew. Math. Mech. **90**, 2000, p. 48.
- [7] I. Stankovic, M. Kröger and S. Hess, Phys. Rev. E, 2003, submitted.
- [8] S. Hess and M. Kröger, Phys. Rev. E **64**, 2001, 011201.
- [9] B. L. Holian, A. F. Voter, N. J. Wagner, R. J. Ravelo, S. P. Chen, W. G. Hoover, C. G. Hoover, J. E. Hammerberg, and T. D. Dontje, Phys. Rev. A **43**, 1991, p. 2655.
- [10] R. A. Johnson, Phys. Rev. B **37**, 1988, p. 3924; R. A. Johnson, Phys. Rev. B **37**, 1988, p. 6121; R. A. Johnson, Phys. Rev. B **39**, 1989, p. 12554.
- [11] M. P. Allen and D. J. Tildesley, Computer Simulations of Liquids, (Oxford Science, UK, 1990)

E-mail address: stankovic@itp.physik.tu-berlin.de (I. Stanković – И. Станковић)